Journal of Molecular Structure 985 (2011) 157–166

Contents lists available at ScienceDirect

Journal of Molecular Structure

journal homepage: www.elsevier.com/locate/molstruc

A comparative study of dynamic NMR spectroscopy in analysis of selected *N*-alkyl-, *N*-acyl-, and halogenated cytisine derivatives

Anna K. Przybył *, Maciej Kubicki

A. Mickiewicz University, Faculty of Chemistry, ul. Grunwaldzka 6, 60-780 Poznań, Poland

ARTICLE INFO

Article history:
Received 23 August 2010
Received in revised form 21 October 2010
Accepted 21 October 2010
Available online 5 November 2010

Keywords:
Cytisine
N-cytisine derivatives
Dynamic NMR spectroscopy
X-ray of cytisine derivatives
Conformational equilibrium

ABSTRACT

New halogenated derivatives of (-)-cytisine were synthesized: 3-bromo-*N*-acetylcytisine, 5-bromo-*N*-acetylcytisine, 3,5-dibromo-*N*-acetylcytisine, 3-iodo-*N*-acetylcytisine, 5-iodo-*N*-acetylcytisine, 3,5-diiodo-*N*-acetylcytisine. Their structures were established on the basis of their NMR spectra and X-ray diffraction method. The crystal structures confirmed the chair conformation of ring C, while in solution all these compounds are in cis–trans conformational equilibrium with ring C in chair and boat conformation. Additionally, the correct X-ray structure of *N*-benzylcytisine was resolved.

1. Introduction

(-)-Cytisine (**1**) is an alkaloid characterised by high biological activity, naturally occurring in plants of the family *Leguminosae*. The compound interacts with the nicotine receptors type α4β2 [1] and therefore, it has been applied in pharmacological treatment of people addicted to nicotine [2] (Tabex®), and moreover, it has been used in investigation of the central nervous system. Cytisine derivatives have been tested as potential drugs for the treatment of Alzheimer's and Parkinson's diseases [1–3] as the hitherto studies have shown that prospective drugs for the treatment of these diseases should also show high affinity with nicotine receptors. Biological activity of (-)-cytisine (**1**) is related to the presence of free electron pairs on the secondary nitrogen atom and a quasi-aromatic ring A. The presence of these elements permits obtaining a number of derivatives [4–7], whose biological activity may be even greater than that of cytisine. On the basis of the hitherto studies of certain cytisine derivatives it has been found that introduction of substituents modifying the molecular structure also changes the pharmacological properties, that is the affinity and inner activity towards certain nACh subtypes and the affinity to ganglionic and centric receptors [7,8].

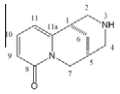

The effect of substitution of N-12 of ring C (in this paper instead of IUPAC numbering traditional numbering is used) leads to the loss of the cytisine activity as a full antagonist towards the receptors α3β4 and α7 nACh, and thus leads to an increase in the selectivity of *N*-substituted cytisine derivatives towards the α4β2 receptors [9]. Moreover, among *N*-substituted cytisine derivatives some compounds with analgesics, activities have been found [10]. Additionally, it has been observed that the substituents in ring at C-3 position increase the affinity to the receptors α4β2, α4β4 i α7, while the C-5 substituents decrease the binding affinity [11].

2. Experimental

2.1. General techniques

Thin layer chromatography (TLC) was performed using aluminium sheets precoated with silica gel 60 F_{254} (Merck). Flash chromatography was carried out on silica gel 60 G F_{254} (Merck). Low- and high-resolution electron ionization (EI) mass spectra (**1**–**7**) were recorded using an AMD Intectra GmbH (Harpsted, Germany) model 402 two-sector mass spectrometer (ionising voltage 70 eV, accelerating voltage 8 kV, resolution 1000 for low-resolution and 10,000 for high-resolution mass spectra).

* Corresponding author. Tel.: +48 61 829 1004; fax: +48 61 829 1505.
E-mail addresses: annaprz@amu.edu.pl (A.K. Przybył), mkubicki@amu.edu.pl (M. Kubicki).

0022-2860/$ - see front matter © 2010 Elsevier B.V. All rights reserved.
doi:10.1016/j.molstruc.2010.10.036

2.2. HPLC separation

Chromatographic methods: LC-DAD analyses were performed on an Agilent 1100 Series liquid chromatographic system consisting of a model G1312A binary pump, a G1379A vacuum degasser, a G1313A autosampler, a G1315B diode-array detector (UV) and Agilent ChemStation data handling program (Agilent Technologies). The reaction mixtures were chromatographed on a 5-μm, 4 mm × 150 mm reversed-phase C18 analytical column (Hypersil GOLD, Thermo Scientific). The column was eluted isocratically for 5 min with water, and then with a gradient from 0% to 30% acetonitrile in 25 min at a flow rate of 1.5 mL/min. Preparative isolation of the products was performed on an Agilent 1200 Series liquid chromatographic system consisting of a model G1312A binary pump, a G1379B vacuum degasser, a G1329A autosampler, a G1315B diode-array detector (UV), G1364C analytical fraction collector and Agilent ChemStation data handling program (Agilent Technologies). Isolation of bromo-*N*-acetyl derivatives of cytisine (**8**–**10**, Scheme 1) was performed on a semipreparative 5 μm, 20 mm × 150 mm (Hypersil GOLD, Thermo Scientific) column. The column was eluted isocratically for 1 min with 20% acetonitrile in water, and then with a gradient from 20% to 50% acetonitrile in 29 min at a flow rate of 4 mL/min. Iodo-*N*-acetyl derivatives of cytisine (**11**–**13**, Scheme 1) were isolated on a semipreparative 5 μm, 10 mm × 250 mm (Hypersil GOLD, Thermo Scientific) column. The column was eluted isocratically for 1 min with 15% acetonitrile in water and then with a gradient from 15% to 40% acetonitrile in 24 min at a flow rate of 4 mL/min.

2.3. NMR spectra

The temperature NMR spectra were measured on a Varian Unity spectrometer (300 MHz), while 1D and 2D NMR spectra were measured in a DMSO-d_6 solution on a Bruker AVANCE 600 (600.31 MHz for ^{1}H and 150.052 MHz for ^{13}C) spectrometer, with a 5 mm triple – resonance inverse probe head (^{1}H/^{31}P/BB) with actively shielded *z* gradient coil (90° ^{1}H pulse width 90 μs, ^{13}C pulse width 13.3 μs). All 2D spectra were acquired and processed using standard Bruker software. Spectral width of 6313.13 and 25,000 Hz were used for 1H and 13C, respectively. Relaxation delays of 2.0 s were used for all 2D experiments and the mixing time 0.8 s for 1H–1H NOESY spectrum was applied. All 2D spectra were collected with 2 K points in F2 and 256 increments (F1) with 4 (g-COSY) and 64 (g-HSQC) transients each and zero filling in F2 to 2048 × 1024 data matrix.

2.4. Compounds

The following alkaloids were studied: (-)-cytisine (**1**) isolated from the seeds of *Laburnum anagyroides* [4], and *N*-acylcytisine (**5**), *N*-propionylcytisine (**6**), and *N*-benzoylcytisine (**7**) were obtained [6] in the reactions with acyl, propionyl and benzoyl chlorides, respectively, while *N*-methylcytisine (**2**) [12], *N*-ethylcytisine (**3**), and *N*-benzylcytisine (**4**) were prepared according to the below procedure.

(-)-Cytisine (**1**, 190 mg, 1 mmol) was dissolved in acetone (10 mL), to which a 10% solution of KOH in acetone (0.25 mL) was added. To get compounds **2**–**4**, to this solution iodomethane, bromoethane or benzylbromide was added dropwise in the amount of 1.5 mmol. The mixture was refluxed for 3 h. The solvent was evaporated and the solid residue was dissolved in water then extracted with CH_2Cl_2 to give crude oil that was purified on Al_2O_3.

The compounds were also characterised by NMR and EI-MS [13].

(-)-Cytisine: (**1**): white crystals, mp 153 °C (compare to lit data [4,6]); IR (KBr, cm^{-1}) 3438 cm^{-1} (*ν*-NH), 2849–2679 cm^{-1} very intensive *trans*-band with maxima at 2803 and 2747 cm^{-1}; 1649 cm^{-1} (*ν* C=O), 1563 and 1540 cm^{-1} (*ν* C=C); NMR in Tables 1 and 2; EI-MS M$^+$ 190 (96%), *m*/*z*: 146 (100%), 147 (99%), 148 (42%), 134 (32%), 160 (29%), 109 (20%). HRMS (EI) calcd. for $C_{11}H_{14}N_2O$ 190.11061, found 190.11011.

N-methylcytisine: (**2**): white crystals, mp 135–136 °C; IR (KBr, cm^{-1}), very intensive *trans*-band with maximum at 2775 and a weak one at 2732 cm^{-1}; 1648 cm^{-1} (*ν* C=O), 1571 and 1550 cm^{-1} (*ν* C=C); NMR in Tables 1 and 2; EI-MS M$^+$ 204 (54%), *m*/*z*: 58 (100%), 146 (15%), 160 (9%). HRMS (EI) calcd. for $C_{12}H_{16}N_2O$ 204.12626, found 204.12745.

N-ethylcytisine: (**3**): Light yellow oil showing no tendency to crystallisation, with HCl, HBr or $HClO_4$; IR (film), very intensive *trans*-band with maxima at 2799 and 2768 cm^{-1}; 1650 cm^{-1} (*ν* C=O), 1566 and 1547 cm^{-1} (*ν* C=C), NMR in Tables 1 and 2; EI-MS M$^+$ 218 (36%), *m*/*z*: 72 (100%), 146 (12%), 160 (9%), 203 (7%). HRMS (EI) calcd. for $C_{13}H_{18}N_2O$ 218.14191, found 218.1470.

Table 1
^{13}C chemical shifts of the compounds **1**–**4** (DMSO-d_6, ppm from TMS).

At C	1	2	3	4
2	162.26	162.18	162.18	163.6
3	115.04	115.29	115.25	116.5
4	138.64	138.77	138.85	138.5
5	103.80	103.77	103.85	104.6
6	152.34	152.13	152.33	151.4
7	34.68	34.43	34.49	35.5
8	25.78	24.66	25.30	25.9
9	27.13	27.22	27.19	26.1
10	49.39	49.58	49.64	49.9
11	52.53	61.71	58.99	59.9
13	53.45	62.18	59.85	60.0
14		45.78	51.25	62.0
15			11.55	–
1′				138.0
2′/6′				128.2
3′/5′				128.1
4′				126.9

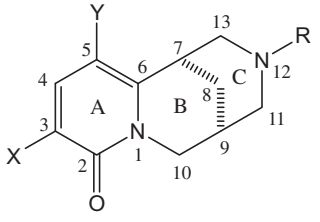

Traditional numbering

	X	Y	R		X	Y	R
1	H	H	H	**8**	Br	H	$COCH_3$
2	H	H	CH_3	**9**	H	Br	$COCH_3$
3	H	H	C_2H_5	**10**	Br	Br	$COCH_3$
4	H	H	$CH_2C_6H_5$	**11**	I	H	$COCH_3$
5	H	H	$COCH_3$	**12**	H	I	$COCH_3$
6	H	H	COC_2H_5	**13**	I	I	$COCH_3$
7	H	H	COC_6H_5				

Scheme 1.

Table 2
^{1}H chemical shifts of the compounds **1–4** (DMSO-d_6, ppm from TMS).

At H	1	2	3	4
3	6.19 dd	6.25 dd	6.19 dd	6.48 dd
4	7.31 dd	7.36 dd	7.32 dd	7.25 dd
5	6.04 d	6.16 d	6.07 d	5.91 dd
7	2.93 s	2.99 ss	3.00 m	2.95–2.93 m
8 α	1.82–1.81	1.64 d	1.68 dt	1.90 m
8 β	m	1.72 d	1.79 dt	1.79 m
9	2.23 s	2.36 ss	2.39 m	2.43 m
10 α	3.68 dd	3.69 dd	3.69 dd	3.88 dd
10 β	3.81 d	3.77 d	3.74 d	4.10 d
11 β	2.89 d	2.12 d	2.81 dd	2.31 d
11 α	2.81 d	2.79 d	2.08 dd	2.36 d
13 α	2.85 d	2.70 d	2.92 dd	2.95–2.93 m
13 β	2.77 dd	2.17 dd	2.19 dd	2.84 d
14		1.99 s	2.22 q	3.42 m
15			0.83 t	–
2′/6′				6.99 bd
3′/5′				7.20–7.14
4′				7.20–7.14

N-benzylcytisine: (**4**): white crystals, mp 133 °C; IR (KBr, cm^{-1}), low intensity *trans*-band at 2875–2737 cm^{-1} with maximum at 2785 cm^{-1}; 1651 cm^{-1} (*ν* C=O), 1566 and 1545 cm^{-1} (*ν* C=C); NMR in Tables 1 and 2; EI-MS M^+ 280 (46%), *m*/*z*: 91 (100%), 134 (89%), 146 (39%), 60 (12%), 189 (12%). HRMS (EI) calcd. for $C_{18}H_{20}N_2O$ 280.15756, found 280.15727.

N-acetylcytisine: (**5**): Yellow oil (lit. crystals, mp. 210 °C [14]), white crystals as $HClO_4$ salt mp 188 °C and as hydrate mp 213 °C; IR (KBr, cm^{-1}), weak *trans*-band with maximum at 2873 cm^{-1}; 1659 and 1617 cm^{-1} (*ν* C=O), 1577 and 1545 cm^{-1} (*ν* C=C); NMR in Tables 3 and 4 and Fig. 2; EI-MS M^+ 232 (100%), *m*/*z*: 146 (61%), 147 (53%), 189 (17%), 148 (14%), 160 (12%). HRMS (EI) calcd. for $C_{13}H_{16}N_2O_2$ 232.12119, found 232.11937.

N-propionylcytisine: (**6**): White crystals, mp 146–147 °C; IR (KBr, cm^{-1}), 2940–2739 cm^{-1} (low intensity *trans*-band with maximum at 2877 cm^{-1}; 1647 and 1609 cm^{-1} (*ν* C=O), 1576 and 1545 cm^{-1} (*ν* C=C); NMR in Tables 3 and 4 and Fig. 2; EI-MS M^+ 246 (76%), *m*/*z*: 147 (100%), 190 (36%), 148 (27%), 57 (27%), 189 (25%), 134 (22%). HRMS (EI) calcd. for $C_{14}H_{18}N_2O_2$ 246.13683, found 246.13571.

N-benzoylcytisine: (**7**): Light yellow oil (lit. crystals, mp. 116 °C [14]), white crystals as $HClO_4$ salt, mp 239 °C; IR (KBr, cm^{-1}), low intensity *trans*-band at 2937–2741 cm^{-1} with maximum at 2866 cm^{-1}; 1651 and 1630 cm^{-1} (*ν* C=O), 1577 and 1545 cm^{-1} (*ν* C=C); NMR in Tables 3 and 4 and Fig. 3; EI-MS M^+ 294 (62%), *m*/*z*: 105 (100%), 77 (42%), 146 (41%), 189 (32%), 147 (12%). HRMS (EI) calcd. for $C_{18}H_{18}N_2O_2$ 294.13684, found 294.13671.

2.4.1. General procedure – synthesis of bromo-derivatives of *N*-acetylcytisine ***8–10***

(-)-*N*-acetylcytisine (**5**, 100 mg, 0.43 mmol, 1 eq.) was dissolved in CH_2Cl_2 (10 mL) and to the solution NBS (0.153 mg; 0.86 mmol, 2 eq.) was added. The mixture was refluxed for 8 h. The solvent was evaporated and the solid residue was dissolved in 10% Na_2CO_3 water and extracted with CH_2Cl_2, dried over anh. $MgSO_4$ and evaporated to give crude oil that was purified on Al_2O_3. The mixture (49% of **8**, 31% of **9** and 20% of **10**) of the products was separated on HPLC (retention time: 17.455; 20.490 and 25.002 respectively for **8**, **9** and **10**).

3-Bromo-N-acetylcytisine: (**8**): mp. 212–214 °C; NMR in Tables 5 and 6; IR (KBr, cm^{-1}), *trans*-band with maximum at 2944 cm^{-1} and 2850 cm^{-1}, 1641 and 1627 cm^{-1} (*ν* C=O), 1583 and 1536 cm^{-1} (*ν* C=C), intensive at 1104 and 1076 cm^{-1}, 1021 and 996 cm^{-1}, 594 and 580 cm^{-1} (*ν* C-Br); EI-MS M^+ 324/326 (49/48%), *m*/*z*: 225/227 (86/100%), 82 (88%), 224/226 (69/67%), 268/270 (29/30%). HRMS (EI) calcd. for $C_{14}H_{17}BrN_2O_2$ 294.13684, found 294.13671.

5-bromo-N-acetylcytisine: (**9**): 209–211 °C; NMR in Tables 5 and 6; IR (KBr, cm^{-1}), *trans*-band with maxima at 2916 cm^{-1} and a weak one at 2870 cm^{-1}; 1657 and 1630 cm^{-1} (*ν* C=O), 1570 and 1524 cm^{-1} (*ν* C=C), intensive bands (*ν* C-Br) at: 1105 cm^{-1}, 1021 and 994 cm^{-1} and 568 cm^{-1}; EI-MS M^+ 324/326 (41/38%), *m*/*z*: 225/227 (99/100%), 82 (97%), 224/226 (50/74%), 189 (52%), 245 (49), 117 (28). HRMS (EI) calcd. for $C_{14}H_{17}BrN_2O_2$ 294.13684, found 294.13671.

3,5-dibromo-N-acetylcytisine: (**10**): mp. 185–186 °C; NMR in Tables 5 and 6; IR (KBr, cm^{-1}), *trans*-band with maxima at 2904 cm^{-1} and a weak one at 2866 cm^{-1}; 1654 and 1627 cm^{-1} (*ν* C=O), 1570 and 1517 cm^{-1} (*ν* C=C) intensive bands (*ν* C-Br) at: 1109 cm^{-1}, 1022 and 999 cm^{-1} and 579 cm^{-1}; EI-MS M^+ 404/406 (29/18), *m*/*z*: 82 (100%), 305/307 (58/24), 303/305 (26/58), 348/350 (27/19), 265/267 (8/27). HRMS (EI) calcd. for $C_{14}H_{16}Br_2N_2O_2$ 294.13684, found 294.13671.

2.4.2. General procedure – synthesis of iodo-derivatives of *N*-acetylcytisine ***11–13***

(-)-*N*-Acetylcytisine (**5**, 100 mg, 0.43 mmol) was dissolved in CH_2Cl_2 (10 mL) and to the solution NIS (0.1935 mg; 0.86 mmol) and benzoyl peroxide was added. The mixture was refluxed for 8 h. The solvent was evaporated and solid residue was dissolved

Table 3
^{13}C chemical shifts of the alkaloids **5–7** (DMSO-d_6, ppm from TMS).

	5			6			7			
At C	42% *cis*	58% *trans*	Coalescence 100 °C	37% *cis*	63% *trans*	Coalescence 100 °C	25 °C	36%* *cis*	64%* *trans*	Coalescence 100 °C
2	162.16	162.08	161.66	162.09	162.04	161.75	162.12	165.34	165.43	161.79
3	115.74	116.06	115.54	115.66	116.00	115.55	116.03	117.18	117.38	115.74
4	138.97	138.79	138.06	138.99	138.79	138.22	138.95	141.82	141.53	138.35
5	104.73	104.63	103.88	104.68	104.61	104.05	104.83	109.15	108.61	104.25
6	149.95	149.59	149.23	149.97	149.65	149.36	149.42	150.97	150.8	149.07
7	33.68	34.31	33.849	33.72	34.25	33.89	34.01	36.02	36.36	38.83
8	25.06	25.24	25.02	25.17	24.81	24.58	25.14	26.52	26.44	25.05
9	27.03	27.00	26.71	26.96	26.66	26.73	26.98	29.33	29.11	26.76
10	47.88	48.62	48.04	48.49	48.61	48.15	48.53	50.21	49.64	48.14
11	48.44	46.86		48.15	47.08		47.42	50.32	49.14	
13	51.61	53.19		50.68	52.22		53.91	54.71	55.86	
15	168.67	168.51	168.06	171.93	171.81	171.63	169.79	173.27	172.82	169.39
16	21.15	20.41	19.84	25.29	25.29	25.14				
17				9.46	9.28	8.68				
1′							135.76	136.55	136.14	135.54
2′/6′							129.23	129.98	129.44	128.755
3′/5′							126.09	127.56	127.45	125.79
4′							128.15	129.96	131.09	127.71

* The spectra have been measured in MeOD at −20 °C.

Table 4
^{1}H chemical shifts of the alkaloids **5–7** (DMSO-d_6, ppm from TMS).

	5			**6**			**7**		
H	42% *cis*	58% *trans*	Coalescence 130 °C	37% *cis*	63% *trans*	Coalescence 130 °C	36%* *cis*	64%* *trans*	Coalescence 130 °C
3	6.19 dd	6.23 dd	6.21 dd	6.20 dd	6.23 dd	6.19 d	6.51 d	6.53 d	6.30 d
4	7.30 dd	7.35 dd	7.30 dd	7.32 dd	7.36 dd	7.29 dd	7.56 dd	7.43 dd	7.40–7.27 m 4H
5	6.13 d	6.22d	6.16 d	6.15 d	6.24 d	6.13 d	6.47 d	6.08 d	5.99 d
7	3.10 bs	3.15 bs	3.12 bs	3.12 bs	3.15 bs	3.21 bs	3.32 m	3.10 m	3.09 bs
8 α	1.95–1.88	1.95–1.91	1.97–1.92	1.98–1.89	1.98–1.89	2.10 m 1H	2.13 m	2.13 m	2.05–1.93 m
8 β	m 4H	m 4H	m 2H	m 4H	m 4 H	1.96 m 1H	4 H	4 H	2 H
9	2.42 m	2.42 ss	2.45 ss	2.43 ss	2.43 ss	2.46 ss	2.38 m	2.63 m	2.98 m
10 α	3.61 d	3.67 d	3.68 d	3.63 m	3.66 m	3.67 dd	3.70 dd	3.86 dd	3.68 dd
10 β	3.81 d	4.00 d	3.94 d	3.92 d	3.80 d	3.92 d	3.94 d	4.28 d	3.98 d
11 β	2.80 d	2.75 d	–	2.81 d	2.77 d	–	3.20 dd	3.15 dd	3.16 d
11 α	4.37 d	4.55 d	–	4.39 d	4.56 d	4.367	4.69 d	4.86 d	4.31 d
13 α	3.28 d	3.41 d	–	3.37 d	3.25 d	–	3.50 dd	3.56 dd	3.30 d
13 β	3.80 d	3.96 d	–	3.85 d	3.99 d	4.109 d	3.79 d	3.68 d	3.95 d
15	1.88 s	1.56 s	1.73 s 3H	1.71 m	2.04 m	1.97 m 3H	–	–	–
16				0.83 t 3H	0.69 t 3H	0.807 t	–	–	–
2'/6'							6.81 d	7.13 d	7.40–7.27 m 4 H
3'/5'							7.38 t	7.28 t	6.90 d 2 H
4'							7.49–7.44 m 4H		7.40–7.27 m 4 H

* The spectra have been measured in MeOD at −20 °C.

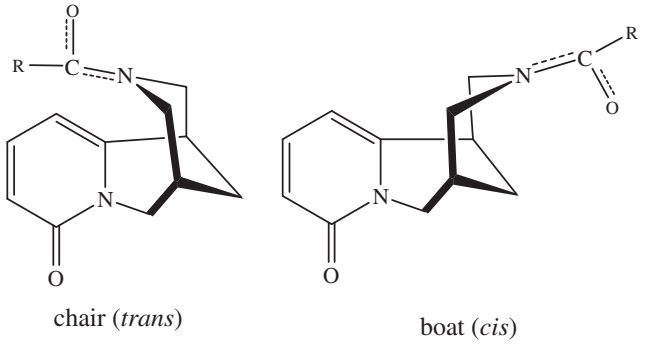

Fig. 1. The possible isomers of *N*-cytisine derivatives Table 3. ^{13}C chemical shifts of the *N*-cytisine derivatives **5–7** (DMSO-d_6, ppm from TMS).

in 10% Na_2CO_3 water and extracted with CH_2Cl_2, dried over anh. $MgSO_4$ and evaporated to give crude oil that was purified on Al_2O_3. The mixture of products (21% of **11**, 2% of **12** and 77% of **13**; without benzoyl peroxide – the mixture of products: 6% of **11**, 91% of **12** and 3% of **13**) was separated on HPLC (retention time: 19.426; 21.760 and 28.266 respectively for **11**, **12** and **13**).

3-iodo-N-acetylcytisine (**11**): mp 213–215 °C; NMR in Tables 5 and 6; EI-MS M^+ 358/359 (100/20%), *m/z*: 272 (91%), 273 (85%), 316/315 (28/26%), 130 (26%), 235 (22%), 82 (23). HRMS (EI) calcd. for $C_{14}H_{17}IN_2O_2$ 294.13684, found 294.13671.

5-iodo-N-acetylcytisine (**12**): yellow oil; NMR in Tables 5 and 6; EI-MS M^+ 358/359 (63/21%), *m/z*: 273/272 (100/68%), 231 (87%), 82 (36), 315/316 (24/17%), 189 (22%). HRMS (EI) calcd. for $C_{14}H_{17}IN_2O_2$ 294.13684, found 294.13671.

3,5-diiodo-N-acetylcytisine (**13**): NMR in Tables 5 and 6; EI-MS M^+ 484/485 (100/23%), 399/398 (57/32%), 357 (42), 441/442 (20/44%), 82 (40), 130 (27), 117 (12). HRMS (EI) calcd. for $C_{14}H_{16}I_2N_2O_2$ 294.13684, found 294.13671.

2.5. X-ray diffraction

Diffraction data were collected at room temperature by the ω-scan technique on an Oxford Diffraction Xcalibur four-circle diffractometer with Eos CCD-detector with graphite-monochromatized Mo Kα radiation (λ = 0.71073 Å). The data were corrected for Lorentz-polarization as well as for absorption effects [15].

Accurate unit-cell parameters were determined by the least-squares fit of 1290 (**9**), 4242 (**6**) and 8692 (**4**) reflections of highest intensity, chosen from the whole experiment. The structures were solved with SIR92 [16] and refined with the full-matrix least-squares procedure on F^2 by SHELXL97 [17]. Scattering factors incorporated in SHELXL97 were used. The function $\Sigma w(F_o^2 - F_c^2)^2$ was minimized, with $w^{-1} = [\sigma^2(F_o)^2 + (A \cdot P)^2 + B \cdot P]$ ($P = [\mathrm{Max}\ (F_o^2, 0) + 2F_c^2]/3$). The final values of *A* and *B* are listed in Table 7. All non-hydrogen atoms were refined anisotropically. The hydrogen atoms were placed geometrically, in idealized positions, and refined as rigid groups with their U_{iso}'s as 1.2 or 1.5 (methyl) times U_{eq} of the appropriate carrier atom.

The hydrogen atoms from the water molecules in **6** were found in the difference Fourier maps and after few cycles of refinement constrained to the so obtained geometry. In **6** the two terminal atoms of the propionyl group were found to be disordered over two positions, the site occupation factors refined at 0.60(1) and 0.40(1); weak restraints were applied to the geometry of the disordered fragment. For **4** and **6** the absolute structure was assigned according to the known parent compounds, for **9** it was additionally confirmed by the value of the Flack parameter. Relevant crystal data are listed in Tables 7 and 8, together with refinement details.

Crystallographic data (excluding structure factors) for the structural analysis have been deposited with the Cambridge Crystallographic Data Centre, Nos. CCDC-751980 (**4**), CCDC-751981 (**6**), and CCDC-751982 (**9**). Copies of this information may be obtained free of charge from: The Director, CCDC, 12 Union Road, Cambridge, CB2 1EZ, UK. Fax: +44(1223)336-033, e-mail: deposit@ccdc.cam.ac.uk, or www: www.ccdc.cam.ac.uk.

3. Results and discussion

Ring A in cytisine and its derivatives assumes a planar conformation, while ring B is in a sofa conformation with the bridging C-8 atom directed out-of-plane, ring C assumes a chair conformation and the nitrogen atom has a free electron pair in the axial position (**1a**). The crystallographic data obtained for the cytisine derivatives have confirmed the trans configuration with respect to the free electron pair on the nitrogen atom [18]. The same positions of the substituents are also indicated by the NMR spectra in solution [19]. Literature data of *ab initio* calculations on cytisine have shown eight conformations, as a result of the presence of two asymmetric carbon atoms C7 and C9 and one amino nitrogen

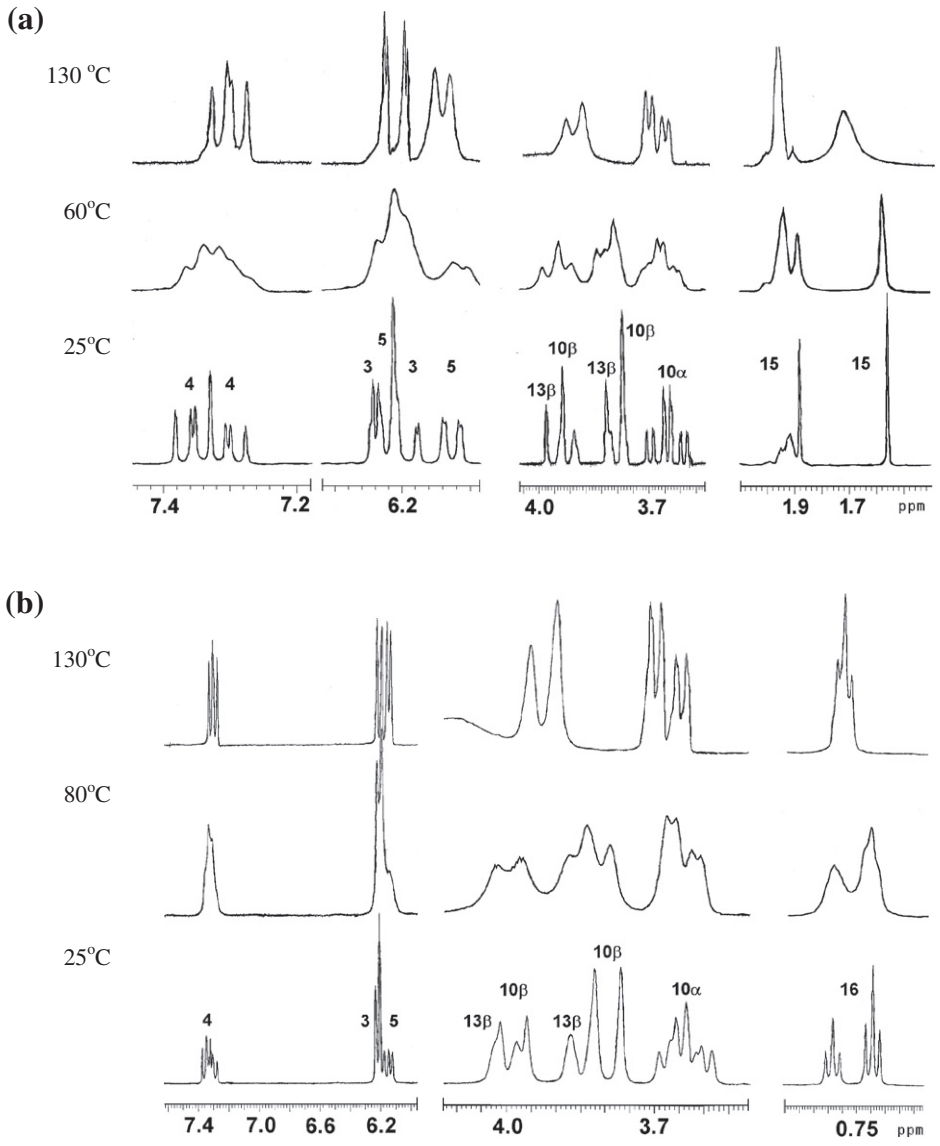

Fig. 2. Fragments of the ^{1}H NMR spectra of compounds **5** (a) and **6** (b) taken at selected temperatures in DMSO-d_6.

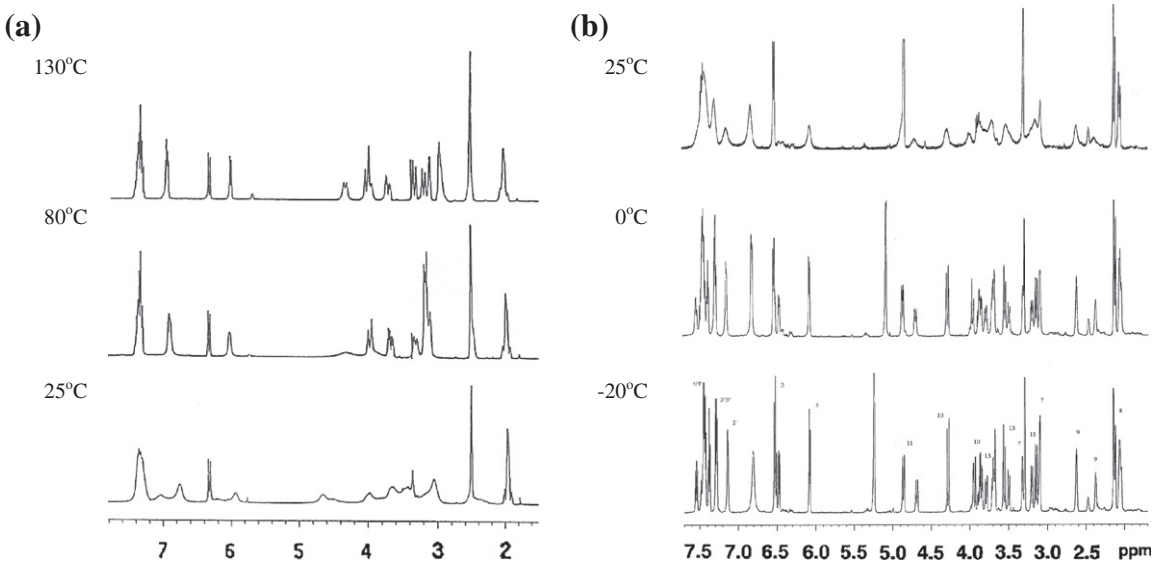

Fig. 3. Fragments of the ^{1}H NMR spectra of **7** taken at selected temperatures (a) in DMSO-d_6; (b) in MeOD.

Table 5
^{13}C chemical shifts of the alkaloids **8–13** (DMSO-d$_6$, ppm from TMS).

	8		9		10		11		12		13	
At *C*	45% *cis*	55% *trans*	48% *cis*	52% *trans*	46% *cis*	54% *trans*	45% *cis*	55% *trans*	46% *cis*	54% *trans*	50% *cis*	50% *trans*
2	158.27	158.22	161.05	160.98	157.57	157.56	159.27	159.3	161.44	161.3	159.15	159.13
3	110.56	110.99	117.30	117.77	112.18	111.68	87.21	87.51	117.84	118.27	89.43	89.93
4	141.08	140.91	142.34	142.14	143.26	143.42	147.6	147.5	147.62	147.43	154.43	154.60
5	105.12	105.06	97.67	97.81	96.89	96.98	106.5	106.4	70.39	70.34	70.94	70.94
6	150.16	149.74	146.64	146.23	146.33	146.80	151.03	150.59	148.62	148.12	148.98	149.55
7	34.12	33.50	33.65	34.33	34.36	33.68	33.41	34.04	37.84	38.46	38.41	37.77
8	24.69	24.85	25.04	25.23	24.93	24.74	24.65	24.82	25.49	25.71	25.21	25.43
9	26.95	26.85	26.58	26.76	26.56	26.79	27.10	27.02	27.05	26.93	27.22	27.06
10	49.92	50.16	49.53	49.45	49.24	51.06	50.10	50.33	49.68	49.61	51.80	51.43
11	47.63	46.75	44.42	46.43	46.36	44.23	47.60	46.76	46.49	44.57	44.43	46.48
13	51.46	52.86	51.16	49.86	51.45	51.06	51.47	52.84	51.21	50.02	51.16	49.44
14	168.75	168.56	168.70	168.31	168.83	168.43	168.8	168.6	168.72	168.32	168.94	168.50
15	21.17	20.52	21.09	20.22	20.36	21.11	21.20	20.53	21.11	20.23	21.19	20.40

Table 6
^{1}H chemical shifts of the alkaloids **8–13** (DMSO-d$_6$, ppm from TMS).

	8		**9**		**10**		**11**		**12**		13	
H δ	47% *cis*	53% *trans*	49% *cis*	51% *trans*	45% *cis*	55% *trans*	46% *cis*	54% *trans*	46% *cis*	54% *trans*	50% *cis*	50% *trans*
3			6.24 d	6.28 d					6.10 d	6.14 d	–	–
4	7.81 d	7.87 d	7.53 d	7.59 d	8.188 d	8.126 d	7.98 d	8.04 d	7.64 d	7.70 d	8.35 s	8.29 s
5	6.16 d	6.25 d					6.03 d	6.12 d				
7	3.15 bs	3.20 bs	3.41–3.36 m 2H	3.37 bs	3.42–3.39 m 3H		3.13 bs	3.18 bs	3.27 bs	3.30 bs	3.29–3.27 m 3H	
8 α	1.98–1.92 m 4 H		2.05–1.95 m 4H		2.023–1.959 m 4H		2.09–1.92 m 4H		2.03–1.96 m 4H		1.96–2.03 m 4H	
8 β												
9	2.44 bs	2.44 bs	2.43 bs	2.43 bs	2.45 bs 2H		2.43 bs	2.43 bs	2.40 bs	2.40 bs	2.40 bs 2H	
10 α	3.79–3.71 m 2 H	3.79–3.71 m 2 H	3.66 dd	3.71 dd	3.80 dd	3.77 dd	3.76 dd	3.71 dd	3.66 dd	3.70 dd	3.76 d	3.79 d
10 β	4.07 d	3.85 d	4.03d	3.81d	3.85 d	4.10 d	3.82 d	4.03 d	3.99 d	3.78 d	3.78 d	4.02 d
11 β	2.81 d	2.76 d	2.78 d	2.78 d	2.79 d	2.79 d	2.81 dd	2.75 dd	2.78–2.74 m 2 H		2.77 bd 2 H	
11 α	4.37 d	4.55 d	4.52 d	4.54 d	4.54 d	4.51 d	4.37 dd	4.54 dd	4.53–4.51 m 2H		4.52 d	4.50 d
13 α	3.97 d	3.81 d	3.41–3.36 m 2H	3.30 d	3.42–3.39 m 3H	3.30 d	3.96 d	3.80 d	3.95–3.86 m 2H		3.87 d	3.95 d
13 β	3.41 dd	3.28 d	3.87d	3.96 d	3.97 d	3.86 d	3.28 dd	3.40 dd	3.40–3.34 m 2 H		3.38 d	3.29–3.27 m 3H
15	1.89 s	1.58 s	1.88 s	1.59 s	1.59 s	1.88 s	1.89 s	1.58 s	1.87 s	1.58 s	1.88 s	1.59 s

atom in the piperidine moiety. The lone pair of electrons on N-12 has the axial or equatorial orientation. There are possible 2 chairs and 2 boats as possible conformations having different *N*-atom lone pair orientation. However, only two of these isomers have the lowest total energy as follows from the calculation, at the AM1 and PM3 levels [20].

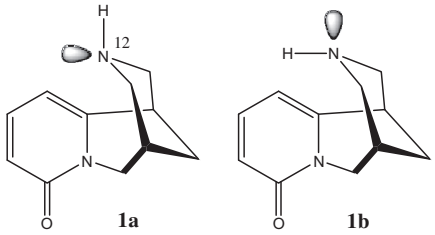

One of them is cytisine α (**1a** – axial orientation of free electron pair) and the other is cytisine β (**1b** – equatorial orientation of free electron pair) which have the most stable structures, separated by a Gibbs energy gap of ca 1.5 kcal/mol [21–23]. The 2 stereogenic C-atoms of these isomers have the same absolute configuration (7R, 9S). The interconversion between these two isomers was confirmed by modelling calculations performed in the solvent for cytisine, where a negligible energy difference (0.007 kcal/mol) between two chair conformations has been found [23]. Hitherto no exact assignment from experimental spectra of the chemical shift signals to the atoms [6] of cytisine (**1**), *N*-methyl- (**2**), *N*-benzyl- (**4**), *N*-acyl- (**5**), *N*-propionyl- (**6**), and *N*-benzoylcytisine (**7**) has been made (Tables 1–4).

The conformer **1a** was identified for the crystal molecule [18]. As follows from the calculations, in the solvents considered both isomers **1a** and **1b** occur in conformational equilibrium [20]. Conformer **1a** seems to be slightly favoured in solvents containing hydrogen bonding donor and/or acceptor groups, whereas conformer **1b** is slightly more stable in the gas phase and apolar solvents [22–24].

The energy difference between chair α (**1a**) as the most stable form and the possible chair β/boat β conformations (Fig. 1) varies in the range of 4.8–6.4 kcal/mol for *N*-alkil derivatives of cytisine [23]. However, the amide derivatives (**5–7**) may occur in solutions in conformational equilibria between two conformations differing in the form of ring C as the chair and boat conformation (Fig. 1). It is due to the rotation of amide group [14,25,26]. The dominant conformation in solution seems to be the same as in the solid state – *trans* (Figs. 4–6). In solutions the amide derivatives of cytisine occur as mixtures of two conformers *trans* and *cis* (Fig. 1 and Tables 3–6), whose presence is manifested as a double set of signals (both in ^{1}H NMR and ^{13}C NMR).

It has been shown that the amide conformers occur in solutions at dynamical equilibrium and their mutual transition is very fast [14,25,26]. However, the lines corresponding to the conformers are recorded in the NMR time scale at room temperature for **5** and **6** (Fig. 2), but for **7** only chemical shifts of carbon atoms (^{13}C NMR) were possible to analyze as the signals of protons (^{1}H NMR) were broad and impossible to indicate any chemical shifts, due to the presence of rotamers (Fig. 3). Therefore, it was necessary to measure the spectrum at lower temperature (^{1}H NMR and ^{13}C NMR in −20 °C). The percentage of the conformers was given

Table 7
Crystal data, data collection and structure refinement.

Compound	**4**	**6**	**9**
Formula	$C_{18}H_{20}N_2O$	$C_{14}H_{18}N_2O_2{\cdot}3H_2O$	$C_{13}H_{15}BrN_2O_2$
Formula weight	280.36	300.35/c	311.18
Crystal system	Orthorhombic	Orthorhombic	Monoclinic
Space group	$P2_12_12_1$	$P2_12_12_1$	$P2_1$
a (Å)	7.185(2)	7.980(2)	7.693(2)
b (Å)	8.585(2)	11.166(2)	10.358(2)
c (Å)	24.980(4)	17.906(3)	8.084(2)
β (°)	90	90	95.56(2)
V (Å^3)	1540.8(6)	1595.5(6)	641.1(3)
Z	4	4	2
d_x (g cm^{-3})	1.21	1.25	1.61
F (000)	600	648	316
μ (mm^{-1})	0.076	0.095	3.202
Θ range (°)	2.51–27.82	2.79–27.81	3.21–28.15
hkl range	$-9 \leqslant h \leqslant 9$	$-10 \leqslant h \leqslant 8$	$-10 \leqslant h \leqslant 8$
	$-11 \leqslant k \leqslant 10$	$-14 \leqslant k \leqslant 14$	$-12 \leqslant h \leqslant 13$
	$-32 \leqslant l \leqslant 32$	$-14 \leqslant l \leqslant 18$	$-10 \leqslant h \leqslant 7$
Reflections			
Collected	16,849	10,237	2499
Unique (R_{int})	2029 (0.020)	2064 (0.032)	1992 (0.018)
With $I > 2\sigma(I)$	1642	1467	1308
No. of parameters	191	212	164
Weighting scheme			
A	0.0461	0.065	0.030
B	0.0829	0	0
$R(F)$ [$I > 2\sigma(I)$]	0.029	0.040	0.034
w$R(F^2)$ [$I > 2\sigma(I)$]	0.072	0.098	0.063
$R(F)$ [all data]	0.040	0.058	0.057
w$R(F^2)$ [all data]	0.081	0.103	0.066
Goodness of fit	1.045	1.020	0.957
max/min $\Delta\rho$ (e Å$^-$)	0.12/−0.12	0.25/−0.13	0.37/−0.34

Table 8
Selected geometrical parameters (Å, °).

	4	**6**	**9**
N1—C2	1.4010(16)	1.386(3)	1.417(5)
N1—C6	1.3717(15)	1.382(3)	1.360(5)
N1—C10	1.4806(15)	1.485(3)	1.483(5)
C2—O2	1.2417(16)	1.255(2)	1.220(6)
C11—N12	1.4621(16)	1.460(3)	1.444(5)
N12—C13	1.4571(15)	1.465(3)	1.452(5)
N12—C14	1.4624(14)	1.324(3)	1.355(6)
C2—N1—C6	122.67(10)	121.74(18)	124.3(4)
C2—N1—C10	114.53(10)	115.26(16)	112.5(4)
C6—N1—C10	122.79(10)	122.88(18)	123.2(4)
C11—N12—C13	110.52(10)	113.5(2)	112.9(4)
C11—N12—C14	112.79(10)	120.3(2)	120.7(4)
C13—N12—C14	111.97(10)	126.1(2)	125.4(4)
N1—C6—C7—C8	32.31(14)	33.7(3)	29.5(5)
C6—C7—C8—C9	−60.14(13)	−61.8(2)	−59.6(5)
C7—C8—C9—C10	64.32(13)	63.8(2)	66.2(5)
C8—C9—C10—N1	−39.69(14)	−37.4(3)	−41.9(6)
C9—C10—N1—C6	10.73(15)	8.3(3)	11.2(6)
C10—N1—C6—C7	−6.92(15)	−6.1(3)	−4.3(5)
C7—C8—C9—C11	−59.54(13)	−61.1(2)	−58.0(5)
C8—C9—C11—N12	60.17(14)	57.9(3)	54.9(5)
C9—C11—N12—C13	−60.35(14)	−54.3(2)	−54.4(5)
C11—N12—C13—C7	60.58(12)	54.0(3)	57.2(5)
N12—C13—C7—C8	−61.33(13)	−58.1(3)	−61.7(5)
C13—C7—C8—C9	60.08(13)	61.3(2)	61.4(5)
C9—C11—N12—C14	172.99(11)	128.6(2)	114.7(5)
C7—C13—N12—C14	−173.22(10)	−129.1(3)	−111.2(5)

according to the integration of the signals in ^{1}H MR and the intensity of the signals in ^{13}C NMR.

The ^{13}C NMR spectra of the compounds studied were taken at temperatures from the range 25 °C up to 100 °C (**5**, **6**, Fig. 2) and in –20 °C to 100 °C (**7**, Fig. 3), while the ^{1}H NMR spectra were taken

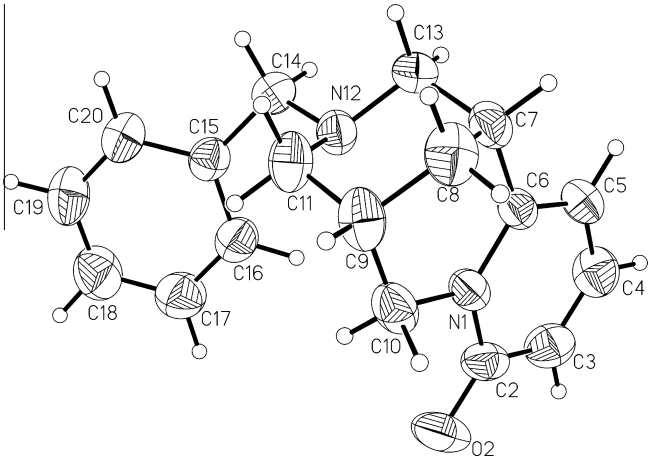

Fig. 4. Perspective view of *N*-benzylcytisine (**4**) with labelling scheme. The ellipsoids are drawn at the 50% probability level, hydrogen atoms are depicted as spheres of arbitrary radii [31].

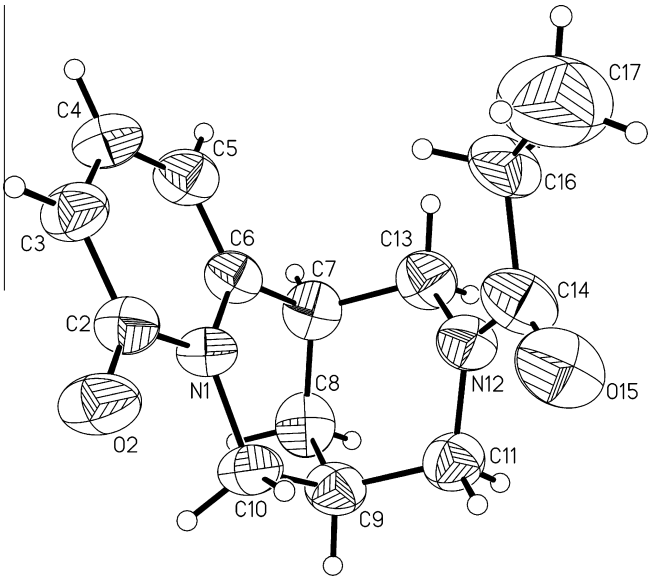

Fig. 5. Perspective view of *N*-propionylcytisine (**6**) with labelling scheme. The ellipsoids are drawn at the 50% probability level, hydrogen atoms are depicted as spheres of arbitrary radii [31]. Only the more occupied alternative for the C16—C17 fragment is shown for clarity.

in the range up to 130 °C, for **7** in the range from −20 °C to 130 °C. The influence of temperature on the spectra is illustrated in Figs. 2 and 3. What seems to be the problem for compounds **5**–**7**, though, are the signals of C-11 and C-13 in ring C that are not visible in the spectra ^{13}C NMR even at 100 °C, which is here called the coalescence temperature. Without doubt they would appear at much higher temperature. However, because of the small amount of the analysed samples and connected with it a long time (4–5 h) of accumulation, we did not decide to increase the temperature of the probe (sonda).

Analyses of the spectra have confirmed the presence of *cis* and *trans* conformers of the compounds studied in DMSO-d_6 solutions and facilitated the assignment of the signals to particular protons and carbon atoms. At the temperature of coalescence of 130 °C for compounds **5** and **6**, the ^{1}H NMR spectra reveal the presence of shared proton signals (Table 4 and Fig. 2). The reason for the overlapping of these signals is the rotation around the single

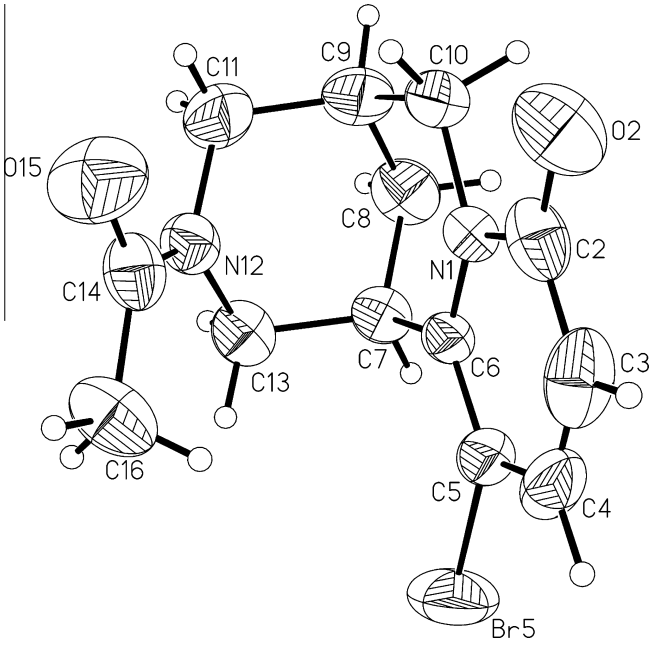

Fig. 6. Perspective view of 5-bromo-*N*-acetylcytisine (**9**) with labelling scheme. The ellipsoids are drawn at the 50% probability level, hydrogen atoms are depicted as spheres of arbitrary radii [31].

Table 9
Hydrogen bond data.

D	H	A	D—H	H···A	D···A	D—H···A
6						
O1 W	H1W1	O15^{i}	0.86	1.93	2.779(3)	173
O1 W	H1W2	O2	0.90	1.97	2.869(2)	174
O2 W	H2W1	O3W^{ii}	0.90	1.85	2.746(3)	175
O2 W	H2W2	O2	0.82	1.99	2.797(2)	169
O3 W	H3W1	O2 W	0.78	2.03	2.796(3)	171
O3 W	H3W2	O1W^{iii}	1.01	1.78	2.784(2)	173
4						
C5	H5	O2^{iv}	0.96	2.42	3.2808(18)	149
C7	H7	O2^{iv}	0.99	2.55	3.3275(17)	135
C8	H8B	O2^{ii}	0.97	2.60	3.5047(17)	157
C19	H19	O2^{v}	0.95	2.58	3.4729(17)	157
9						
C10	H10A	O15^{vi}	0.97	2.55	3.348(6)	140
C11	H11B	Br5^{vii}	0.97	2.94	3.811(5)	150
C16	H16B	O2^{viii}	0.96	2.32	3.258(6)	167

Symmetry codes: $^{i}1-x,\ -1/2+y,\ 1/2-z$; $^{ii}-1/2+x,\ 1/2-y,\ 1-z$; $^{iii}1+x,\ y,\ z$; $^{iv}x-1,\ y,\ z$; $^{v}2-x,\ 1/2+y,\ 3/2-z$; $^{vi}1-x,\ 1/2+y,\ 1-z$; $^{vii}1-x,\ 1/2-y,\ -z$; $^{viii}x,\ y,\ -1+z$.

C—N bond leading to the averaging of the interactions of the group —N—C=O with the rest of the molecule. The chemical shift assignment was facilitated by the two-dimensional spectra indicating that the carbon atom signal of the carbonyl group in the *cis* conformer appeared at a lower magnetic field, while in the *trans* conformer this signal appeared at a higher magnetic field [26]. Similar relations were observed for the *cis* and *trans* isomers of *N*-acyl- and *N*-alkyl- substituted of the amino acid derivatives [27]. However, there are some exceptions in the chemical shifts of C-3, C-7, C-13 in compounds **5**, **6** and **7** and also C-10 in **5** and **6** (Table 3).

On the basis of the signal intensities (^{13}C NMR, Table 3) and integration (^{1}H NMR, Table 4), it is possible to calculate percent contributions of a given conformer in the mixture analysed. The percent contents of the *cis* and *trans* conformers at equilibrium in a DMSO-d_6 solution of compounds **5** and **6** at +25 °C, and of **7** at

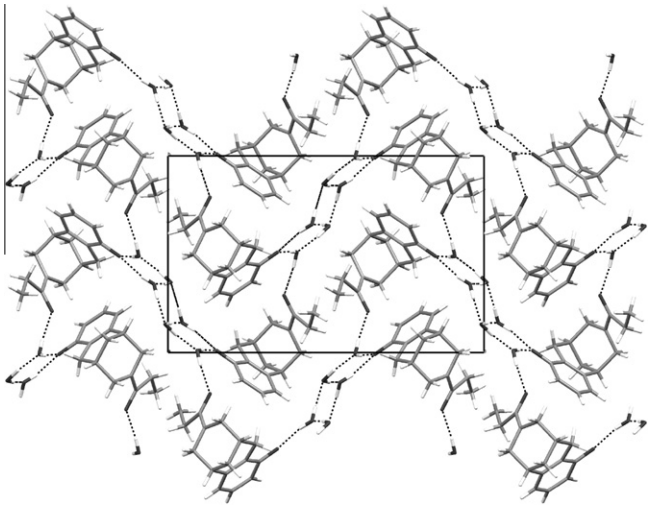

Fig. 7. The crystal packing of **6** as seen along the *x*-direction. Hydrogen bonds are drawn as dashed lines [34].

−20 °C in MeOD solution (it was necessary to change the solvent because DMSO freezes below 19 °C) are given in Tables 3 and 4. And indicated, the percentage of isomer *trans* increases with the more bulky substituents at N-12 (for **5**, **6** and **7** the contribution of *trans* conformer is 58%, 63% and 64%). The temperature spectra taken of particular alkaloids evidence the same percent contribution of the conformers in solution at the beginning of the experiment (25 °C) and after cooling down to the temperature of analysis. Therefore, as a result of increasing temperature no changes apart from an increase in the speed of rotation around the C—N bond take place in the solution.

Additionally, knowing the ^{1}H and ^{13}C NMR data, the population of the conformers studied and the coalescence temperature T_c, it is possible to calculate the free energy of activation ΔG of the process of transition between these two conformers *cis* and *trans* using the Eyring formulae and chart ($\log[X/2\pi(1 \pm \Delta P)]$ and $\log[X/2\pi(1 - \Delta P)]$) [28].

$$G_A = RT_c \ln\left[\frac{k}{h\pi}\left(\frac{T_c}{\partial v}\right)\left(\frac{X}{1-\Delta P}\right)\right]$$

$$G_A = 4.57T_c\left[10.62 + \log\frac{X}{2\pi(1-\Delta P)} + \log\frac{T_c}{\delta v}\right]$$

$$G_B = 4.57T_c\left[10.62 + \log\frac{X}{2\pi(1+\Delta P)} + \log\frac{T_c}{\delta v}\right]$$

$$G_B = RT_c \ln\left[\frac{k}{h\pi}\left(\frac{T_c}{\partial v}\right)\left(\frac{X}{1+\Delta P}\right)\right]$$

In these formulae: R is the gas constant, k is the Boltzmann constant, h is the Planck constant, T_c temperature of coalescence, ΔP difference in the populations of the conformers, $\delta\upsilon$ difference in the chemical shifts of the signals of the two conformers at a very slow transition at a temperature much lower than T_c, here at 25 °C [Hz].

The energy of transition between these two conformers of *N*-acetylcytisine (**5**) ΔG was calculated to be $\Delta G = 2.8$ kcal/mol (^{1}H NMR at $T_c = 130$ °C) and $\Delta G = 2.5$ kcal/mol (^{13}C NMR at $T_c = 100$ °C), while for *N*-propionylcytisine (**6**) ΔG was calculated as 3.8 kcal/mol (^{1}H NMR at $T_c = 130$ °C) and 3.5 kcal/mol (^{13}C NMR at $T_c = 100$ °C). In the case of benzoylcytisine (**7**) ΔG was calculated as 4.8 kcal/mol (^{1}H NMR at $T_c = 130$ °C) and 4.4 kcal/mol (^{13}C NMR at $T_c = 100$ °C).

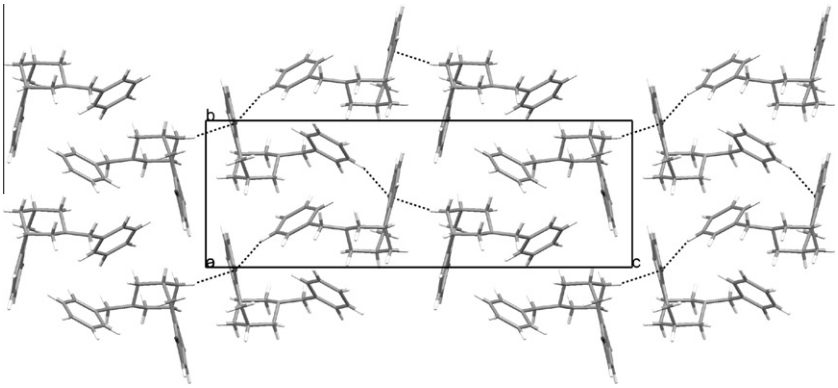

Fig. 8. The crystal packing of **4** as seen along the *x*-direction. Weak directional interactions C—H···O are drawn as dashed lines [34].

4. X-ray structures of the representative molecules 4, 6 and 9

Up to now, the numerous X-ray structural studies of cytisine N-derivatives had been published [19,23,29]. In this work, the structures of the chosen compounds introduced in this paper has been analysed. Figs. 4–6 show the perspective views of the molecules of **4**, **6** and **9**, respectively. Tables 7 and 8 lists some relevant geometrical parameters. Additionally, we decided to correct the information given by Bouquillon et al. [30] about the structure of *N*-benzylcytisine (**4**). In the paper the authors introduced the X-ray structure of *N*-benzyltetrahydrocytisine instead of *N*-benzylcytisine (**4**). For this reason we introduced the X-ray structure as Fig. 4. And the data according to this molecule are given in Tables 7 and 8.

The geometry of the molecules is quite similar, the bond lengths and angles are close to the typical values (Tables 7 and 8). The overall conformation of molecules is similar to those of the other cytisine derivatives (cf. Figs. 4–6). Rings A are almost planar, maximum deviation from the least-squares plane is 0.017(1) in **4**, 0.005(2) Å in **6**, and 0.005(3) in **9**. Rings B have the half-chair conformations, with five atoms almost coplanar and the bridgehead C8 atom significantly out of this plane, by 0.7244(16) Å (**4**), 0.733(8) Å (**6**) and 0.735(7) Å (**9**), and rings C are close to the ideal chair conformation. This structure can be also described using the language of the asymmetry parameters [32], which measure the deviation from the ideal symmetry of the certain conformation. The ideal half-chair should possess C_s symmetry, and the appropriate asymmetry parameter for *B*, ΔC_s^{N1} are quite small for **6** it is 2.7°, for **4** its value is 5.4° and for **9** it is 9.0°. The deviation from the ideal chair symmetry of D_{3d} in ring C depends on the nature of the substituent. When the first carbon atom is sp^3 hybridized, ring C is almost ideal chair, for **4** the maximum values of the appropriate asymmetry parameters are ΔC_s^{C7} of 0.95° and ΔC_2^{7-8} of 1.30°.

A similar situation was observed lately for instance in the structure of *N*-methyl-2-thiocytisine [33]. When there is the sp^2-hybridized carbon atom, as in **6** and **9**, the deviations from the ideal symmetry are more significant; the maximum values of the asymmetry parameters in **6** are: ΔC_s^{C9} of 5.0° and ΔC_2^{C9-11} of 7.0°, ad for **9** ΔC_s^{C9} of 5.1° and ΔC_2^{C8-9} of 6.9°.

The compound **6** crystallizes as trihydrate. The main packing force in this case is provided by the hydrogen bonds involving water molecules and both carbonyl oxygen atoms of **6**. Table 9 lists the hydrogen bond data as well as the details of weaker hydrogen-bond-like interactions for the remaining two compounds. In the crystal structure of **6** there are hydrogen bonded layers of **6** and water molecules, these layers are further interconnected by other O—H···O hydrogen bonds (Fig. 7). In **4** and **9** there are no strong hydrogen-bond donors, so the crystal structures are determined by close packing, van der Waals interactions and some weak but directional, and to some extent specific interactions C—H···O and C—H···Br (Table 9 and Figs. 8 and 9).

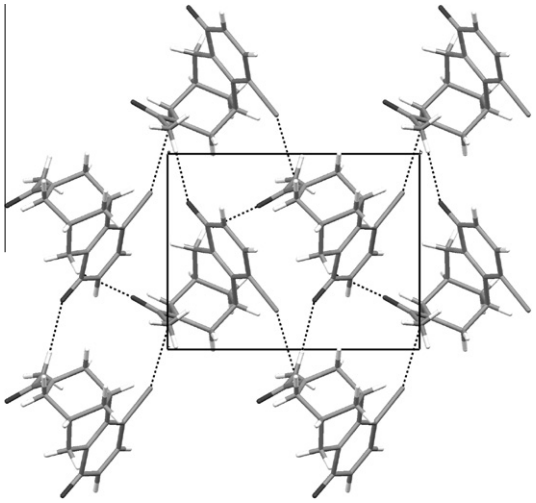

Fig. 9. The crystal packing of **9** as seen along the *x*-direction. Weak directional C—H···O and C—H···Br interactions are drawn as dashed lines [34].

5. Conclusions

The 1D and 2D NMR spectra (300 MHz and 600 MHz) of the cytisine derivatives studied were taken and the chemical shifts were assigned to the corresponding atoms in their molecules. The results were found to be in agreement with the literature data as the chemical shift δ [ppm] corresponding to the carbonyl atoms of the amide group at higher [ppm] correspond to the *cis* conformer, while those at lower [ppm] correspond to the *trans* conformer.

On the basis of the intensity of the lines assigned to the proton and carbon atoms the percent contributions of particular conformers of compounds **5** and **6** in DMSO-d_6 solution at 25 °C, and respectively in MeOD at −20 °C for **7** were determined. The activation energy ΔG of the transition between these two conformers *cis* and *trans* of *N*-acylcytisine, *N*-propionylcytisine and *N*-benzoylcytisine was calculated using the Eyring formulae [28].

In this paper, the misunderstanding of the name and the structure mentioned in literature [30] was corrected and the correct X-ray structure of *N*-benzylcytisine was presented.

Aknowledgement

This project has been supported by the Scientific Research Committee of Poland Grant No. N N312 187835.

References

[1] (a) M.G. LeSage, D. Shelley, J.T. Ross, F.I. Carroll, W.A. Corrigall, Pharmacol. Biochem. Behav. 91 (2009) 461;
(b) C. Botuha, C.M.S. Galley, T. Gallagher, Org. Biomol. Chem. 2 (2004) 1825;
(c) J. Zhang, J.H. Steinbach, Brain Res. 959 (2003) 98;
(d) D.J. Anderson, S.P. Arneric, Eur. J. Pharmacol. 253 (1994) 261.

[2] (a) A. Einarson, S. Riordn, Eur. J. Clin. Pharmacol. 65 (2009) 325;
(b) J.-F. Etter, R.J. Lukas, N.L. Benowitz, R. West, C.M. Dresler, Drug Alcohol Depend. 92 (2008) 3.

[3] (a) M. Mousavi, E. Hellström-Linahl, Neurochem. Int. 54 (2009) 237;
(b) J.A. Abin-Carriquiry, G. Costa, J. Urbanavicius, B.K. Cassels, M. Rebolledo-Fuentes, S. Wonnacott, F. Dajas, Eur. J. Pharmacol. 589 (2008) 80.

[4] E. Marriere, J. Rouden, V. Tadino, M.-C. Lasne, Org. Lett. 8 (2000) 1121. Supporting Information http://pubs.acs.org.

[5] (a) C.C. Boido, F. Sparatore, Il Farmaco 54 (1999) 438;
(b) P. Imming, P. Klaperski, M.T. Stubbs, G. Seitz, D. Gundisch, Eur. J. Med. Chem. 36 (2001) 375;
(c) O. Nicolotti, C.C. Boido, F. Sparatore, A. Carotti, Il Farmaco 57 (2002) 469.

[6] J. Rouden, A. Ragot, S. Gouault, D. Cahard, J.-C. Plaquevent, M.-C. Lasne, Tetrahedron: Asymmetry 13 (2002) 1299.

[7] C.C. Boido, T. Vito, F. Sparatore, Il Farmaco 58 (2003) 265.

[8] Y.E. Slater, L.M. Houlihan, P.D. Maskell, R. Exley, I. Bermudez, R.J. Lukas, A.C. Valdivia, B.K. Cassels, Neuropharmacology 44 (2003) 503.

[9] (a) U.S. Makhmudov, K.K. Turgunov, B. Tashkhodzhaev, V.A. Saprykina, Kh.M. Shakhidoyatov, Chem. Nat. Comp. 44 (2008) 46;
(b) M.S. Frasinyuk, V.I. Vinogradova, S.P. Bondarenko, V.P. Khilya, Chem. Nat. Comp. 43 (2007) 590;
(c) D.V. Shishkin, E.R. Mukhamed'yarova, N.Z. Baibulatova, V.A. Dokichev, Yu.V. Tomilov, Chem. Nat. Comp. 43 (2007) 293;
(d) D.V. Shishkin, A.R. Shaimuratova, A.N. Lobov, N.Z. Baibulatova, L.V. Spirikhin, M.S. Yunusov, N.S. Makara, N.Zh. Baschenko, V.A. Dokichev, Chem. Nat. Comp. 43 (2007) 190;
(e) I.V. Nagorichna, A.S. Ogorodniichuk, M.M. Garazd, V.I. Vinogradova, V.P. Khilya, Chem. Nat. Comp. 43 (2007) 10.

[10] (a) T.S. Rao, L.D. Correa, R.T. Reid, G.K. Lloyd, Neuropharmacology 35 (1996) 393;
(b) T.W. Seale, S. Singh, G. Basmadjan, Neuroreport 9 (1998) 201.

[11] (a) Y.E. Later, L.M. Houlihan, P.D. Maskell, R. Exley, I. Bermúdez, R.J. Lukas, A.C. Valdivia, B.K. Cassels, Neuropharmacology 44 (2003) 503;
(b) R. Varas, V. Valdés, P. Iturriaga-Vásquez, B.K. Cassels, R. Iturriaga, J. Alcayaga, Brain Res. 1072 (2006) 72;
(c) J.A. Abin-Carriquiry, G. Costa, J. Urbanavicius, B.K. Cassels, M. Rebolledo-Fuentes, S. Wonnacott, F. Dajas, Eur. J. Pharm. 589 (2008) 80.

[12] V. Galasso, A.K. Przybył, V. Christov, B. Kovač, F. Asaro, E. Zangrando, Chem. Phys. 325 (2006) 365.

[13] A.K. Przybył, W. Prukała, Rapid. Commun. Mass Spectrom. 22 (2008) 261.

[14] N.P. Abdullaev, U.S. Makhmudov, B. Tashkhodzaev, G. Genzhemuratova, M.G. Levkovich, K.M. Shakhidoyatov, Chem. Nat. Compd. 45 (2009) 837.

[15] Oxford Diffraction. CrysAlis PRO (Version 1.171.33.36d). Oxford Diffraction Ltd., 2009.

[16] A. Altomare, G. Cascarano, C. Giacovazzo, A. Gualardi, J. Appl. Cryst. 26 (1993) 343.

[17] G.M. Sheldrick, Acta Cryst. A64 (2008) 112.

[18] A.A. Frezer, D.J. Robins, G.N. Sheldrake, Acta Cryst. C43 (1987) 1119.

[19] P. Mascagni, M. Christodoulou, W.A. Gibbons, K. Asres, J.D. Phillipson, N. Niccolai, S. Mangani, J. Chem. Soc. Perkin Trans. II (1987) 1159.

[20] E. Górnicka, E.D. Raczyńska, Talanta 57 (2002) 609.

[21] E.D. Raczyńska, M. Makowski, E. Górnicka, M. Darowska, Int. J. Mol. Sci. 6 (2005) 143.

[22] E. Górnicka, M. Makowski, M. Darowska, E.D. Raczyńska, Pol. J. Chem. 75 (2001) 1483.

[23] G. Bombieri, F. Meneghetti, R. Artali, B. Tasso, C. Canu Boido, F. Sparatore, Chem. Biodivers. 5 (2008) 1867.

[24] E. Górnicka, J.E. Rode, E.D. Raczyńska, B. Dasiewicz, J.Cz. Dobrowolski, Vib. Spectrosc. 36 (2004) 105.

[25] T.V. Khakimova, O.A. Pukhlyakova, G.A. Shavaleeva, A.A. Fatykhov, E.V. Vasil'eva, L.V. Spirikhin, Chem. Nat. Comp. 37 (2001) 356.

[26] G. Palla, G. Predieri, P. Domiano, Tetrahedron 42 (1986) 3649.

[27] (a) J.S. Davies, J. Chem. Soc. Perkin Trans. II 11 (1978) 1157;
(b) H.L. Maia, K.G. Orrell, H.N. Rydon, J. Chem. Soc. Perkin Trans. II (1976) 761.

[28] (a) E. Wyrzykiewicz, D. Prukała, J. Heterocyclic Chem. 35 (1998) 381;
(b) H. Shanan-Atidi, K.H. Bar-Eli, J. Phys. Chem. 74 (1970) 961;
(c) W.E.K. Wynne-Jones, H. Erying, J. Chem. Phys. 3 (1935) 492.

[29] (a) O.A. Nurkenov, A.M. Gazaliev, K.M. Turdybekov, A.B. Bukeeva, I.V. Kulakom, Zh. Obshch. Khim. (Russ.) (Russ. J. Gen. Chem.) 73 (2003) 1015;
(b) A.A. Freer, D.J. Robins, G.N. Sheldrake, Acta Crystallogr. Sec. C: Cryst. Struct. Commun. 43 (1987) 1119;
(c) M.K. Ibraev, D.M. Turdybekov, S.D. Fazylov, K.M. Turdybekov, A.M. Gazaliev, T.S. Zhivotova, Zh. Org. Khim. (Russ.) (Russ. J. Org. Chem.) 40 (2004) 752;
(d) B. Tashkhodjave, K.K. Turgunov, A.G. Tojiboev, U.S. Makhmudov, T.F. Ibragimov, V.A. Saprykina, Kh.M. Shakhidoyatov, J. Inclusion Phenom. Macrocyclic Chem. 61 (2008) 71;
(e) V.N. Khrustalev, K.A. Krasnov, J. Mol. Struct. 828 (2007) 188;
(f) O.A. Nurkenov, A.M. Gazaliev, B. Ibragimov, A.Kh. Zhakina, K.M. Turdybekov, Zh. Obshch. Khim. (Russ.) (Russ. J. Gen. Chem.) 66 (1996) 1212;
(g) Atta-Ur-Rahman, A. Pervin, M.I. Choudhary, N. Hasan, B. Sener, J. Nat. Prod. 54 (1991) 929;
(h) U.S. Makhmudov, K.K. Turgunov, B. Tashkhodzhaev, V.A. Saprykina, Kh.M. Shakhidoyatov, Khim. Prir. Soedin (Russ.) (Chem. Nat. Compd.) (2008) 375;
(i) I.V. Kulakov, O.A. Nurkenov, D.M. Turdybekov, A.A. Ainabiev, K.M. Turdybekov, A.M. Gazaliev, Khim. Prir. Sordin (Russ.) (Chem. Nat. Compd.) (2009) 56.

[30] S. Bouquillon, J. Rouden, J. Muzart, M.-C. Lasne, M. Hervieu, A. Leclaire, B. Tinant, C.R. Chimie 9 (2006) 1301.

[31] Siemens, Stereochemical Workstation Operation Manual. Release 3.4. Siemens Analytical X-ray Instruments Inc., Madison, Wisconsin, USA, 1989.

[32] W.L. Duax, D.A. Norton, Atlas of Steroid Structures, Plenum, New York, 1975. p. 16.

[33] A.M. Owczarzak, A.K. Przybył, M. Kubicki, Acta Cryst. E66 (2010) o1942.

[34] C.F. Macrae, I.J. Bruno, J.A. Chisholm, P.R. Edgington, P. McCabe, E. Pidcock, L. Rodriguez-Monge, R. Taylor, J. van de Streek, P.A. Wood, J. Appl. Cryst. 41 (2008) 466.